Experimental Study of Thermocapillary Flow in The Half-Zone Liquid Bridge of Low Prandtl Number Fluid

By
Satoshi Matsumoto[1], Hitoshi Hayashida[1], Atsuki Komiya[1], Hidesada Natsui[2], and Shinichi Yoda[1]

Abstract: The experimental study on thermocapillary convection of low Prandtl number fluid was carried out to understand transition behavior to oscillatory flow. The half-zone liquid bridge of molten tin was formed between hot and cold disks in high vacuum chamber (10^{-5} Pa). The three radiation thermometers were used to measure the free surface temperature at a different azimuthal location at the same time. In addition, the temperature distribution at interface between liquid bridge and cold disk was measured by using very fine thermocouples. In order to detect the transition point and to make clear the oscillation mode more precisely, the temperature measurement system was developed.

It could be detected that the steady thermocapillary convection changes to oscillatory under certain condition. The observed phenomena of transition processes after the oscillatory onset were revealed by comparing to numerical result done by Imaishi *et al.*. The effect of aspect ratio (L/r) on critical Marangoni number was investigated. The critical Marangoni number decreases with increasing the aspect number. This behavior agrees with numerical simulation done by Imaishi *et al.* qualitatively except for region of smaller aspect ration.

Since the echo signal from the tracer had the very small bad SN ratio, in order to raise the SN ratio, signal processing technique was examined. Consequently, the noise which originates in the shoe by the subtraction processing technique was removable. And the SN ratio could be improved by the addition processing by repetition measurement, and the SN ratio improved about 3 times by calculation supposing actual measurement. The A/D converter and the system controller were manufactured in the 3D-UV measurement unit.

1. INTRODUCTION

It is well known that thermocapillary convection changes its flow motion by increasing the control parameters such as temperature difference. In the case of liquid bridge of low Prandtl number fluid, it is numerically predicted that an axisymmetric steady flow transit to asymmetric 3D steady flow. After that, convection becomes oscillatory under certain condition. Namely, the thermocapillary convection of low Prandtl number fluid go through two transition points to become an oscillatory flow. We need to understand the transition mechanism because the oscillatory flow has an undesirable effect on the crystal growth of semiconductors by the floating zone methods, which lead to striations of the dopant in the crystal. The previous studies, in which a

[1] Japan Space Exploration Agency, 2-1-1, Sengen, Tsukuba, Ibaraki 305-8505, Japan
[2] Advanced Engineering Services Co. Ltd., 1-6-1, Takezono, Tsukuba, Ibaraki 305-0032, Japan

half zone liquid bridge have been often used as a model configuration of the floating zone, have shown that flow and temperature fields were governed by dimensionless parameter of Marangoni (Ma) or Reynolds (Re) number defined as follows:

$$Ma \equiv \frac{|\sigma_T|\Delta T L}{\mu \kappa} \quad (1\text{-}1),$$

$$Re \equiv \frac{Ma}{Pr} \quad (1\text{-}2),$$

σ_T is a temperature gradient of surface tension, ΔT is a temperature difference between hot and cold disks, L is a characteristic length of the fluid, μ is dynamic viscosity, α is thermal diffusivity, and Pr is Prandtl number of the fluid. In this study, a radius (a) of the liquid bridge is used as a characteristic length.

In higher Pr number fluids, it was experimentally proved that a transition from axisymmetric steady to 3D oscillatory flow occurs at a critical Marangoni number (Ma_c). On the other hand, it was numerically predicted that thermocapillary flow in a low Pr number had two transition points [1], [2]: That is, transition from axisymmetric to 3D steady will occur at a first bifurcation point (Ma_{c1}), and transition from 3D steady to oscillatory at a second one (Ma_{c2}). The prediction needs to be experimentally proved.

A detail experiment around the bifurcation point, in which even the Ma_{c2} is predicted to be in the order of 10^1 for a Pr =0.01 liquid bridge [3], is required to prove the transition behavior of Marangoni convection. However, many studies have been conducted at a Marangoni number that is far from the Ma_{c2} because those have mainly focused on a contribution to produce a high quality single crystal from a molten metal.

Nakamura et al. [4], [5] measured a surface temperature fluctuation with a thermocouple in a molten silicon column of 10mm in diameter and 10mm in length, and found that a frequency of the fluctuation was 0.1Hz at a temperature difference of 100K. However, the imposed temperature difference was far from the second bifurcation point. Han et al. [6] experimentally investigated thermocapillary convection in a liquid bridge of mercury. Free surface fluctuations were measured by a non-contacted diagnostic system, and they found the Ma_{c2}, detecting it to be 900 with a frequency around 5Hz. Quite recently, Yang and Kou [7] reported the onset point of temperature fluctuation and its frequency (Ma_{c2}=194 and 1.1Hz) of a molten tin column by the contacted diagnostic, *i.e.* J-type thermocouple. However, disturbances on the flow and temperature field are caused by a thermocouple which contacts with a fluid and a thermocouple often acts as a cold spot which makes it a complicated temperature gradient along a free surface. It should be noted here that there is no successful experiment to verify the transition behavior of thermocapillary flow by a non-contact diagnostic even nearby the Ma_{c2}.

The goal of present study is to understand the transition phenomena of thermocapillary flow by means of an experimental approach and comparative study with the numerical works in this research group.

The experimental efforts began to select a fluid material for a low Pr number liquid bridge in 1998 [8]. The selected material was molten tin of which Pr number is identical with that of molten silicon (Pr =0.01). Therefore, we can directly compare our experimental result with available experimental and numerical results of molten silicon because the identical Pr number means to show the same fluid dynamic behavior. Moreover,

molten tin as a test fluid has an experimental advantage in a detection of Ma_{c2} compared to molten silicon. Since the melting point of tin is much lower than that of silicon, there is no need to use an infrared image furnace for melting a tin sample, which was used for a molten silicon experiment [4] and [5], and an electric heater is applicable to melt it. Thus, it is expected that the surface temperature of a molten tin column can be measured by a non-contact diagnostic with relatively low noise level. The high purity iron was selected as solid material to sustain a liquid bridge because of the reason that moderate wettability and low reactivity against molten tin is required for the solid material [8].

On the other hand, the selected test fluid has a thermodynamic disadvantage which the oxygen partial pressure is extremely low at the equilibrium between molten tin and tin oxides (SnO and SnO_2) near the temperatures for the low Pr experiment (about 570-770K), resulting in suppressing the thermocapillary flow by the formation of an oxide film over a surface of the melt. However, in 1999, we have successfully overcome the difficult problem of oxidation over the tin surface [9]. Consideration concerning the surface science of tin led us to design of a unique experiment apparatus where a clean surface of molten tin can be obtained by the Ar^+ ion etching method and sustained under the high vacuum condition (about 10^{-6} Pa) during an experiment. The performances of the experiment apparatus were already confirmed. In 1999, a non-contact measurement technique of the surface temperature has been also developed to detect small amplitude of temperature fluctuation at around the Ma_{c2} [9]. It was also confirmed that the radiation thermometer which is equipped with the PbS photo detector and combined with the attachments to obtain a high signal-to-noise ratio such as CaF_2 optical pass filter and an isotropic graphite panel had the sufficient temperature resolution to detect the Ma_{c2} with high accuracy. It was concluded that those unique considerations and devices undoubtedly lead us to a success of detecting the transition to oscillatory flow of the low Pr fluid without any flow disturbances.

Compared with the conventional transparent fluid used for a high Pr number experiment, a low Pr number fluid has another experimental difficulty: It is impossible to observe an internal flow field for opaqueness of a low Pr fluid. In order to overcome this problem, a novel visualization technique using an ultrasonic transducer with a high heat resistance has been experimentally studied for an internal flow field measurement since 1999 [9]. The visualization technique also requires a development of a unique balloon-like tracer. A critical condition on the Ma_{c1} and a detail structure of oscillatory flow will be clarified by this measurement technique.

The experimental results with molten tin obtained in 2000 are significant for the thermocapillary convection of a low Pr fluid. As predicted in the last issue [9], we have succeeded in detection of the transition to oscillatory flow by the surface temperature measurement without any flow disturbances. The flow transition was verified by comparison of the experimentally obtained Ma_{c2} and frequency of surface temperature fluctuation with the numerical results, and by a surface flow visualization experiment directly [10]. The effect of the liquid bridge geometry on the Ma_{c2} and oscillation frequency was further investigated and discussed [11]. The following results are described in this study:

(1) Experimental verification of surface temperature measurement (in-house activity)
(2) Detection of transition phenomena to oscillatory flow (in-house activity)
(3) Effect of aspect ratio on the critical condition and flow structure (in-house activity)

(4) Numerical simulation for the specific case (collaboration with Kyushu University)

(5) in-situ measurment of surface tension of the molten tin

(6) Development of measuring technique of internal flow field (entrusted to Toshiba Co.)

(7) Development of visualization tracer (collaboration with Kagoshima Prefectural Institute of Industrial Technology and partly entrusted to NTT Advanced Technology Co.)

2. TRANSITION PHENOMENA TO OSCILLATORY THERMOCAPILLARY FLOW OF MOLTEN TIN

2.1 Experimental Setup

The experimental apparatus is shown in Figs 2-1, 2-2, 2-3 [8,9,10]. It consists of a liquid bridge formation part, a measurement region, a sample supplying system and a sample cleaner. The liquid bridge was formed by sandwiching between a pair of pure iron disk (purity: 99.5%). All experiments were done in the ultra high vacuum conditions, which were under 10^{-5}Pa, to keep clean sample surface and less heat loss of molten tin liquid bridge. To impose the temperature difference, the lower disk was cooled by helium gas and the upper disk was heated by an electric resistant heater. The electric heaters were not controlled by PID (Proportional, Integral and Derivative) control to circumvent the temperature hunting phenomena. The temperature difference was gradually increased from around 0K to above the onset. An imposed ΔT was measured with the thermocouples embedded at near the end face of the disks.

Solid tin (purity: 99.999%) is melted in a quartz tube as illustrated in Fig. 2-2. The melt is supplied onto the lower disk *via* the capillary portion (1mm in inner diameter) of the quartz tube where bulk oxide in the crude fluid can be removed. For further purification, Ar^+ ion etching method was applied and the ion gun designed for surface cleaning was installed in the chamber. Surface temperature of the liquid bridge was measured with a radiation thermometer, in which PbS photo detector was installed, mounted on outside of the chamber.

The lower disk was optimized to measure the temperature field of liquid bridge as shown in Fig.2-3. The measurement of temperature field was necessary to understand the oscillatory thermocapillary convection. Because of the motion of temperature field was coincided with the one of oscillatory flow. It has been inserted some ϕ 0.3 mm K-type thermocouples (TC) sheathed a stainless steel in these 0.35 mm-holes. The top of thermocouples was adjusted the same position as lower disk plane.

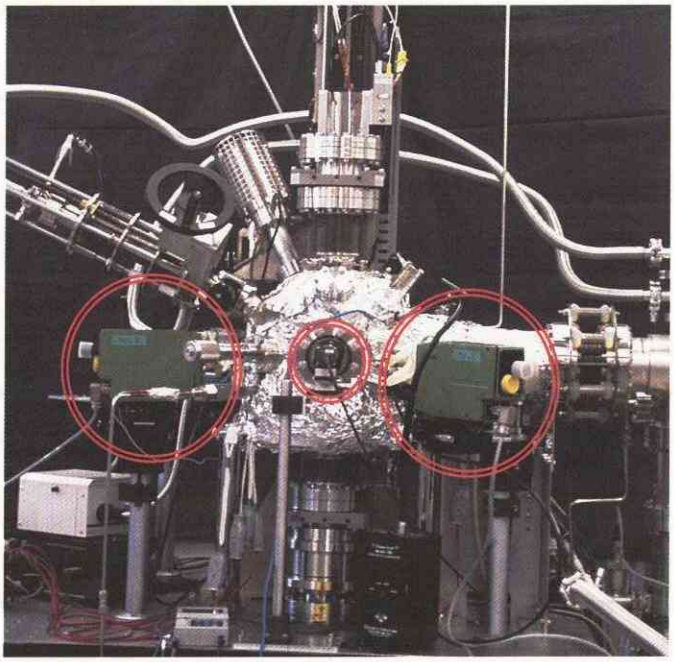

Fig. 2-1 Experimental equipment

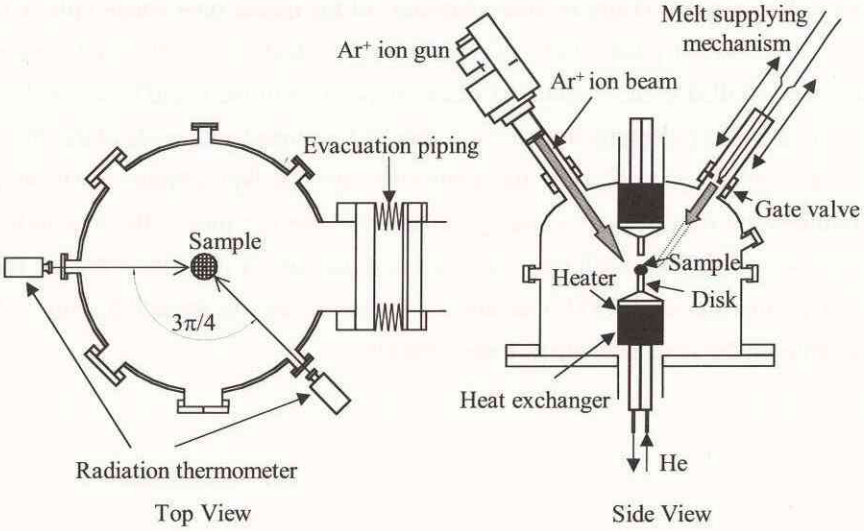

Fig. 2-2 Schematic diagram of experimental equipment

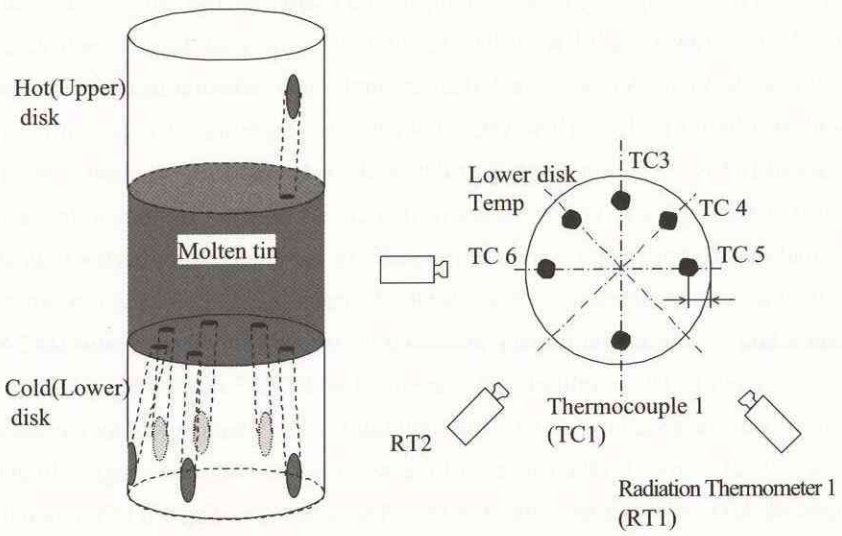

Fig. 2-3 Temperature measurement points
(a) Schematic diagram of tin liquid bridge and disks
(b) Lower disk surface and positions of radiation thermometers

2.2 Improvement of Experimental Techniques

(1) Purification of liquid bridge

The purity of formed liquid bridge is very important because an oxide on a free surface can change the surface tension. Therefore the purification of supplied molten tin should be done. As mentioned above, the experimental equipment already has a sample cleaner system, such as Ar^+ ion gun, high vacuum chamber, and sample supplying capillary tube. In addition of these, a stainless steel mesh filter was installed in the capillary tube last year. It can stain off the crude fluid, which is mainly oxide, from supplying molten tin. The capillary tube for sample supplying system is shown in Fig.2-4. Molten tin flows from left fat to right thin parts. In the case of no filter, a white powder-like sludge adhered on the inwall of slim part of capillary tube. On the other hand, the mesh filter worked very efficiently, because no sludge can be found below the filter in Fig. 2-4. Consequently, the liquid bridge could be refined.

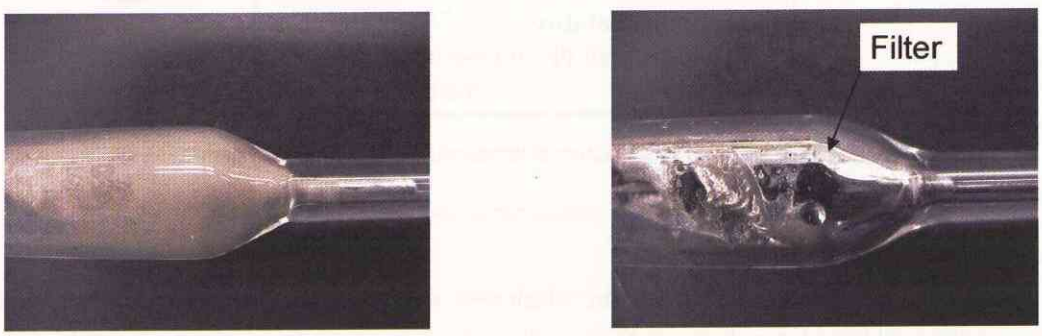

(i) without filter (ii) with 0.1 mm mesh filter

Fig. 2-4 Improvement of sample supplying tube

2.3 Improvement of temperature measurement system

In case of low Prandtl thermocapillary flow, the temperature change or fluctuations at transition points is very small (eg. 0.01 K for the first transition, 0.1 K for the second transition). Therefore, the sensitivity of temperature measurement system must be high. As mentioned, thermocouples and radiation thermometers are used to detect the temperature field of a liquid bridge. However, a temperature resolution of radiation thermometer used in this experiment is about 0.3 K. It is not enough to detect fluctuations. So, we used several thermocouples. Output signal from thermocouples is very tenuous in this case. E-type thermocouples that could produce relatively large thermal electromotive force were employed. In this experiment higher temperature resolution is important rather than absolute temperature. Such weak electromotive force of thermocouples was amplified. The voltage corresponding to thermocouple was produced by the DC signal generator (DC-SG). The signal from thermocouple was input to DC amplifier with the signal of DC-SG differentially in order to remove DC component. This signal was increased to 5×10^4 times amplitude. The frequency of temperature fluctuation was estimated in order of several Hertz. So the low-pass filter was used to reduce the higher frequency noise. The signals were digitized by A/D converter and stored in PC. The schematic diagram of temperature measurement system is shown in Fig. 2-5. The temperature resolution of less than 0.01 K achieved by using this measurement system.

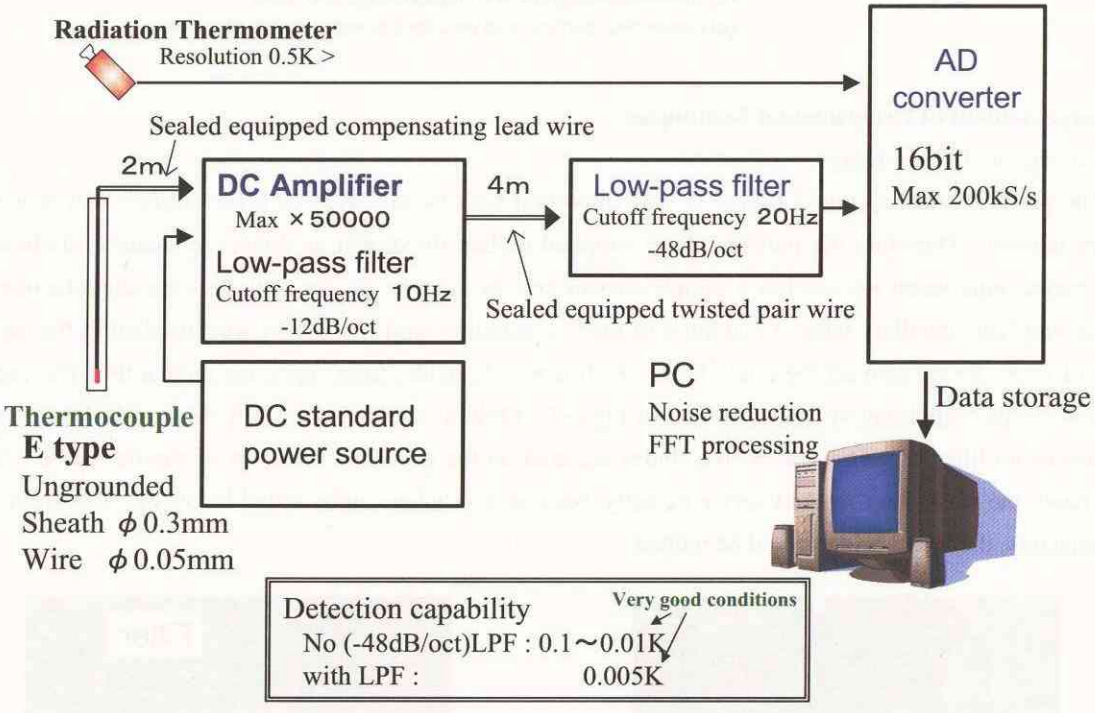

Fig. 2-5 Schematic diagram of temperature measurement system

2.4 Observation of first transition

Fig. 2-6 shows time variations of temperature which were measured by three thermocouples located in cold disk. Temperature suddenly jumped around 1510 s. Since there could not be any oscillatory behavior after the temperature jump, this seems to be the first transition point which have been predicted by numerical simulation. In this case, aspect ratio of liquid bridge was 1.8, a temperature difference, ΔT, was 1.7 K, and Marangoni

number was 11. From the relation between thermocouple position and temperature change, the mode structure seems to be unity and the cold spot located in the center of liquid bridge near cold disk moved to peripheral region as shown in Fig. 2-7.

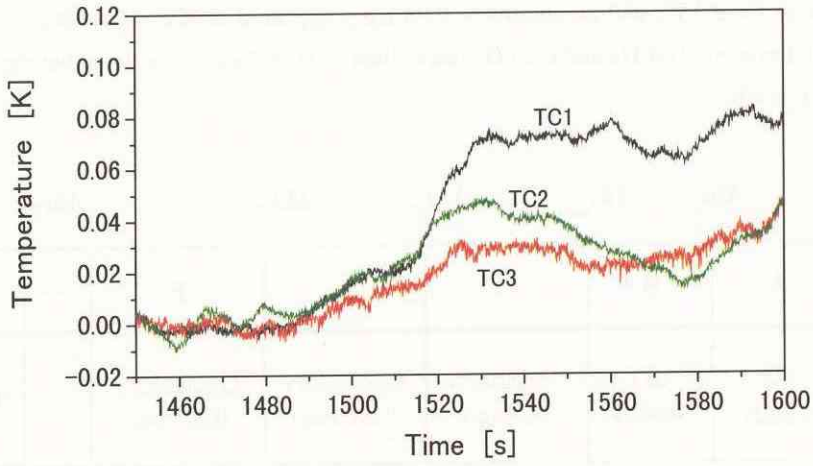

Fig. 2-6 Time variation of temperature at first transition point

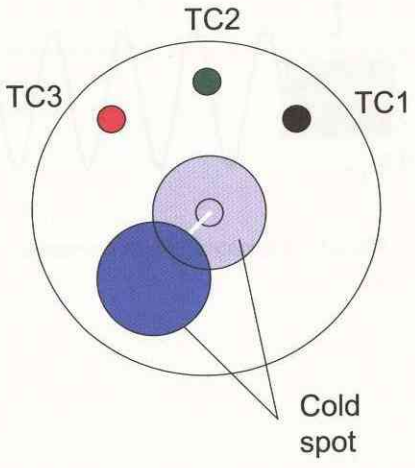

Fig. 2-7 Schematic of mode structure and movement of cold spot near cold disk

2.5 Transition process of oscillatory flow

It was estimated by numerical simulation that several transitions occur after the onset of oscillatory flow. We divided each region as shown in Fig. 2-8. The onset of oscillation is called the second critical Maragoni number Ma_{c2} or $Ma_{c2\text{-}1}$. The transitions after $Ma_{c2\text{-}1}$ were named $Ma_{c2\text{-}2}$ and $Ma_{c2\text{-}3}$ sequentially. In previous experiment, $Ma_{c2\text{-}1}$ could not detect because its signals was very small. Improvement of temperature measurement method provides us precise observation of just onset point.

An oscillatory transition was detected with larger temperature difference after an occurrence of first transition. The temperature fluctuation measured by thermocouple is shown in Fig. 2-9. At first, relatively higher frequency fluctuation with a frequency $f = 1.2$ Hz appeared at $Ma_c = 43$ (see Fig. 2-9 (i)). The amplitude

of this fluctuation was about 0.1 Kp-p (Peak to Peak). It was considered that this transition was the second critical point since the frequency was same order of numerical result which was 2.5 Hz. In this case, Mac2-2 could not detected. In Fig. 2-9 (ii), (iii), the lower and middle frequency fluctuations were depicted in case of As=1.2. The lower frequency with f = 0.02 Hz and an amplitude 0.4 Kp-p appeared at Ma = 82 ($Ma_{c2\text{-}2}$). The middle frequency with f = 0.3 Hz and an amplitude 0.08 Kp-p appeared at Ma = 125 ($Ma_{c2\text{-}3}$). The frequencies by numerical simulation were 0.04 Hz and 0.25 Hz respectively. Therefore, we believe that the transition process was detected very precisely.

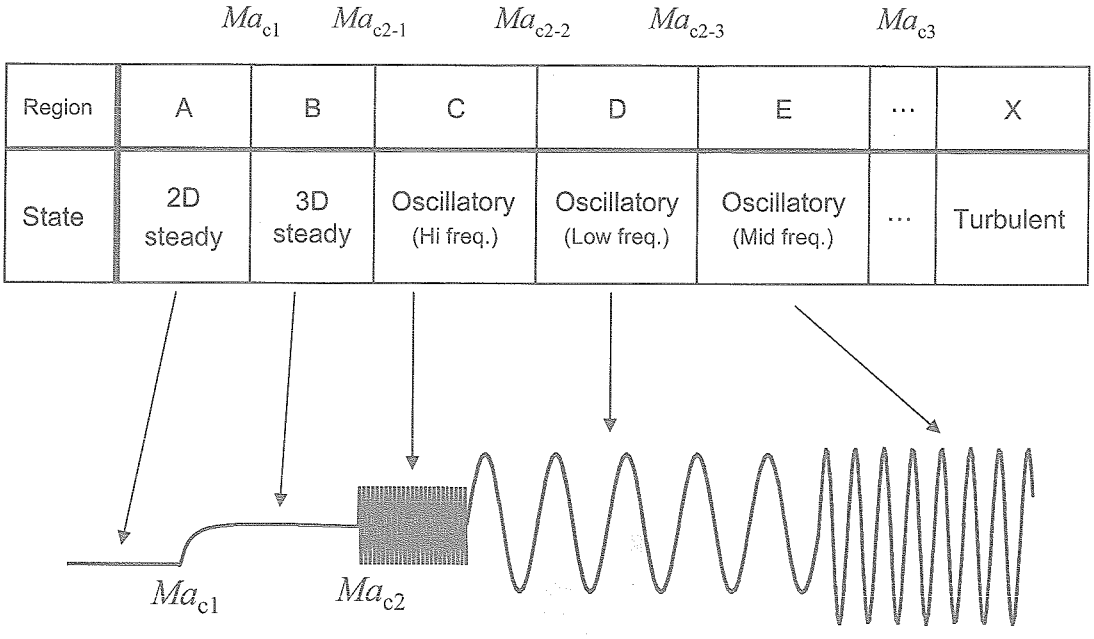

Fig. 2-8 Estimated transition process

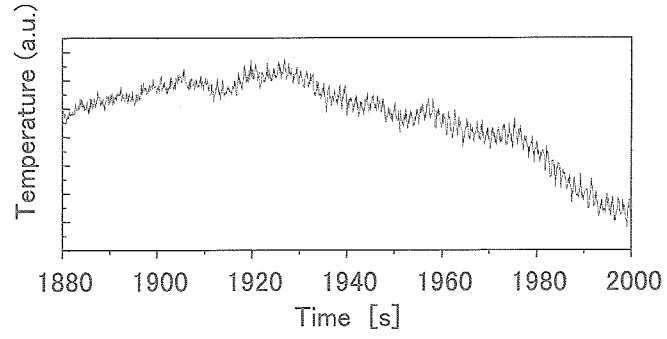

$f \sim 1.2$ [Hz] (Exp.)
2.5 [Hz] (Simulation)

(i) Higher freq.

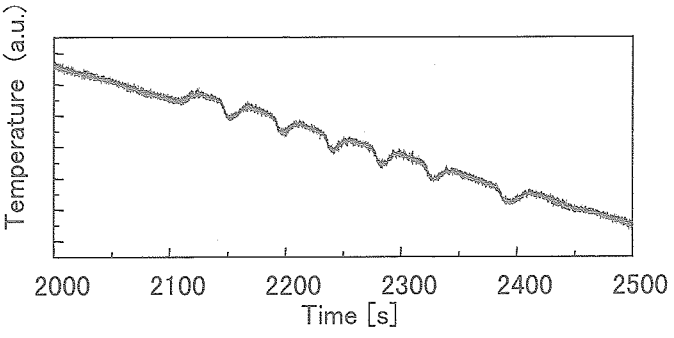

$f \sim 0.02$ [Hz] (Exp.)
0.04 [Hz] (Simulation)

(ii) Lower freq.

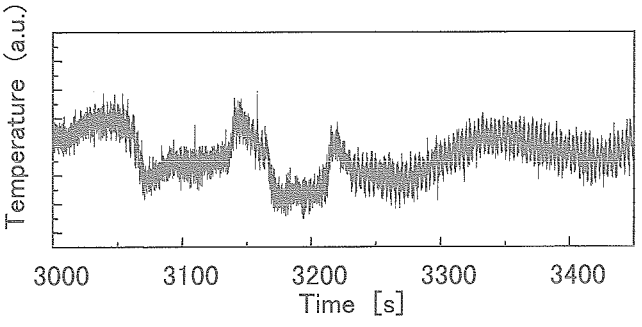

$f \sim 0.30$ [Hz] (Exp.)
0.25 [Hz] (Simulation)

(iii) Middle freq.

Fig. 2-9 Detected temperature fluctuation

2.6 Effects of aspect ratio

(1) Experimental conditions

The disk diameters from 3.0mm to 7.0mm were used in order to covering liquid column with aspect ratio (*As*: height/radius) from 0.8 up to 2.2. This range almost corresponds to calculated range of numerical simulation by Imaishi *et al.* [13]. Heights of the liquid column were adjusted in from 1.5 mm to 4.5 mm at all the experimental cases, minimizing the dynamic bond number *Bd* (*Bd*<1).

$$Bd \equiv \frac{\rho g \beta L^2}{\sigma_T} = \frac{Ra}{Ma}$$

where ρ, is density, g gravitational acceleration, β volumetric expansion coefficient, σ_T temperature gradient of surface tension, L the height of the liquid column and Ra is Rayleigh number. However the static bond number B_0 is larger than unity, volume ratio or diameter ratio (D/D_{max}), surface shape is almost straight.

$$B_0 = \frac{\rho g L^2}{\sigma}$$

In every case, temperature difference (ΔT) was imposed at certain changing rate. In some cases, ΔT was reduced after transition in order to measure surface temperature behavior when damping. Since the control of changing rate of ΔT (dΔT/dt) is very difficult, there were some widths on them. Influence of ramping rate of temperature difference, dΔT/dt on transition was discussed in previous report. The dΔT/dt ranging from 0.4 to 2.1 K/min has no influence in the critical Marangoni number. Therefore we controlled the dΔT/dt around 0.5 K/min.

(2) Ma_c as a function of aspect ratio

In order to make clear the influence of aspect ratio on Ma_{c2}, the onset of oscillatory thermocapillary flow using liquid columns with As from about 0.8 to 2.2 are investigated. In the case of experimental work in this case, Ma_{c2} is determined by the temperature difference at the onset of low frequency oscillation. It seems reasonable because the Ma_{c2} at the second transition point was slightly 10 % higher than the first point.

The Ma_{c2} as a function of As, which was experimentally and numerically obtained by Imaishi *et al.* [13], are shown in Fig. 2-10. The estimated oscillation mode is also described in this figure. The experimental Ma_{c2} in the range of As higher than about 1.2 well corresponds to numerical one. The experimental Ma_{c2} increases with decreasing of As monotonically. In contrast, the numerical Ma_{c2} has a peak at As = 1.2 and the one slightly decreases when As in the range of 1.0 = As = 1.2 decreases. The experimental results showed that the Ma_{c2} (As = 1.3), which was obtained using the liquid column with relative large radius and the one lied on relative low Marangoni number, was obtained by the experimental conditions at small dΔT/dt. We will make clear the reason why the experimental critical Marangoni number in the smaller aspect region differs from the numerical result in near future.

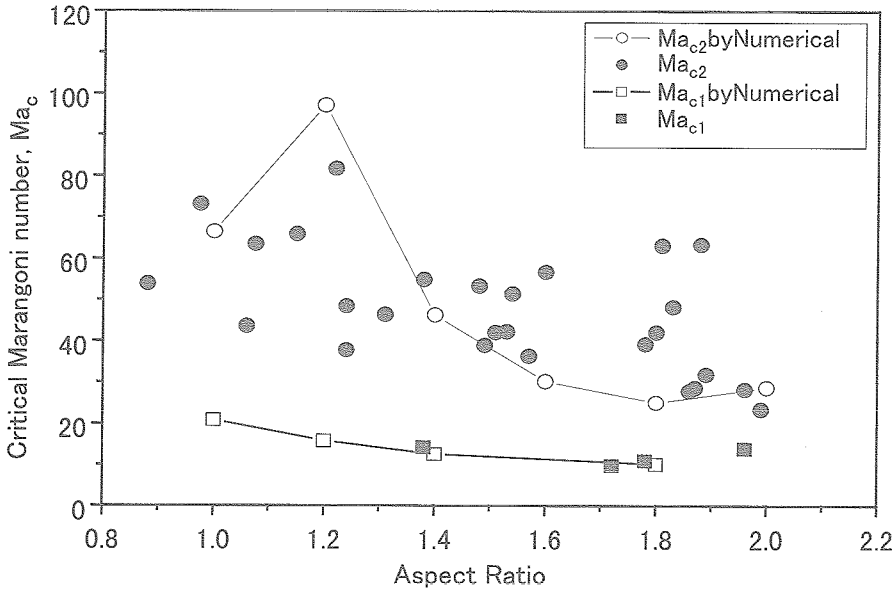

Fig.2-10 Dependence of Marangoni number on aspect ratio

3. DEVELOPMENT OF 3D-UV AND TRACER PARTICLE

3.1 Development of 3D-UV

In 1999, a test for evaluating delectability of $LiNbO_3$ (LN) transducer was performed at room temperature using a drilled glass target, which simulated balloon tracers in molten tin. It was predicted that a detectable minimum diameter of tracer was 100-200 μm [9].

In 2000, a test for evaluating sensitivity of transducer at high temperature conditions same as actual thermocapillary experiment was performed in molten tin. High spatial resolution was obtained in the direction of wave propagation. Numerical simulation was performed in order to check visualization performance of ongoing sensor-design. It was confirmed that tracers in molten tin liquid bridge could be visualized [17].

In 2001, the transducer with 3 × 3 LN element was made and checked its sensitivity. The sensor was verified the stability after heat treatment up to 500 °C which is same as actual thermocapillary experiment. The frequency band of oscillator was selected to get the clear echo signal. The optimal frequency was 6 to 14 MHz wide-band. [18].

In 2002, the Fe-Ni/SB plating practical tracer was manufactured and coexistence nature with melted tin was checked in actual thermocapillary condition. By C-scan probe measurement, the ultrasonic echo from the particle in tin [19].

3.1.1 Study of the signal processing technique

The Fe and Ni plated Shirasu-ballons (Fe-Ni/SB) which is the tracer particle used by this 3D-UV system is very small. Therefore, the reflective echo signal measured is a very low level. Moreover, a shoe is attached in the transducer in order to protect an LN element to the molten tin. While the echo measured with a shoe declines, the sound noise by the inside reflection of a shoe is added. For realization of 3D-UV system, it becomes very important to acquire the echo signal from the tracer by sufficient the signal to noise (SN) ratio. Then, the signal processing technique for extracting the echo signal was studied.

An example of the echo from the imitation tracer in molten tin in the 1999 fiscal year (hollow stainless steel ball) is shown in Fig.3-1. The imitation tracer was moved in molten tin and the echo was measured. Fig.3-1 showed time series data and average value. In this result, the echo is hidden by the noise and distinction of it is clearly impossible.

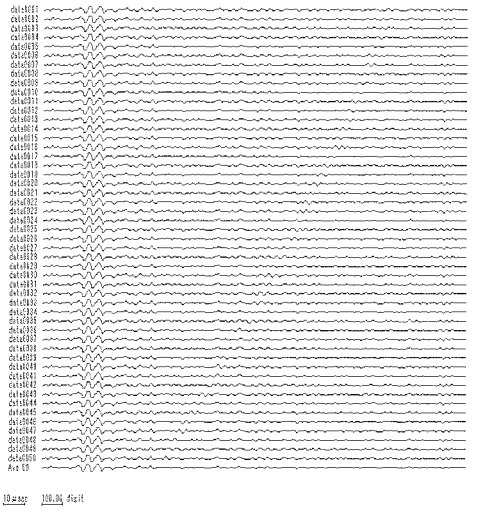

Fig.3-1 The echo from the tracer obtained by the test using molten tin

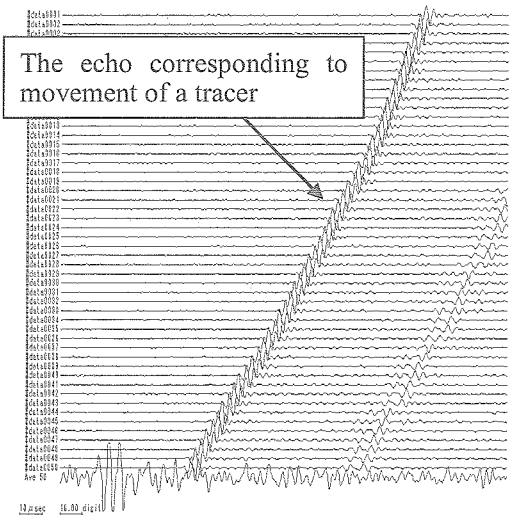

Fig.3-2 The result of subtraction processing

Therefore, it is necessary to raise SN ratio by signal processing, and to extract the echo. The result which removed the noise from the shoe by signal processing is shown in Fig.3-2. Subtraction processing of the noise was carried out from the echo, and the SN ratio was raised. The average value of the echo of much measurement was made into the noise resulting from the shoe.

Next, the improvement effect in the SN ratio by other techniques was examined. The speed of the ultrasonic wave used for 3D-UV is very high-speed compared with the move speed of the tracer. Then, if much measurement with a short repetition cycle is performed and addition processing is carried out, improvement in the SN ratio will be attained. In repetition measurement, a difference arises in the echo waveform measured by movement of the tracer for every measurement. Then, the numerical simulation considered the influence of echo signal change. In calculation, the tracer echo waveform was created using the sin wave of two cycles, and the imitation noise was created from the random number. And addition processing of the 100 data which mixed and made the echo and the noise was carried out. Moreover, it was assumed that analog-to-digital (A/D) conversion was carried out 1/10 cycle of the cycle T of the ultrasonic wave. When the echo is the SN ratio equal 0, the result calculated as that in which the echo waveform carried out time change is shown in Fig. 3-3. In Fig. 3-3, if time change of the echo becomes large, the improvement effect in the SN ratio of addition processing will decrease. Thereby, the scope of the improvement effect in the SN ratio by addition processing became clear. The case where it applied to an actual examination was considered. If the repetition cycles of transmission and reception of the ultrasonic wave were assumed to be 100 μsec, the total measurement time will be set to 0.01 sec. And if the maximum speed of SB tracer was assumed to be 50 mm/sec, time change of the echo signal will be set to about 0.4 μsec. Since the frequency of the ultrasonic wave to be used is 5MHz, time change of this echo signal is equivalent to 2T. Improvement in about 3 of the SN ratio is expectable from Fig. 3-3 with addition processing. Moreover, if the repetition cycle of transmission and reception of the ultrasonic wave is shortened, it will become possible to raise the SN ratio further.

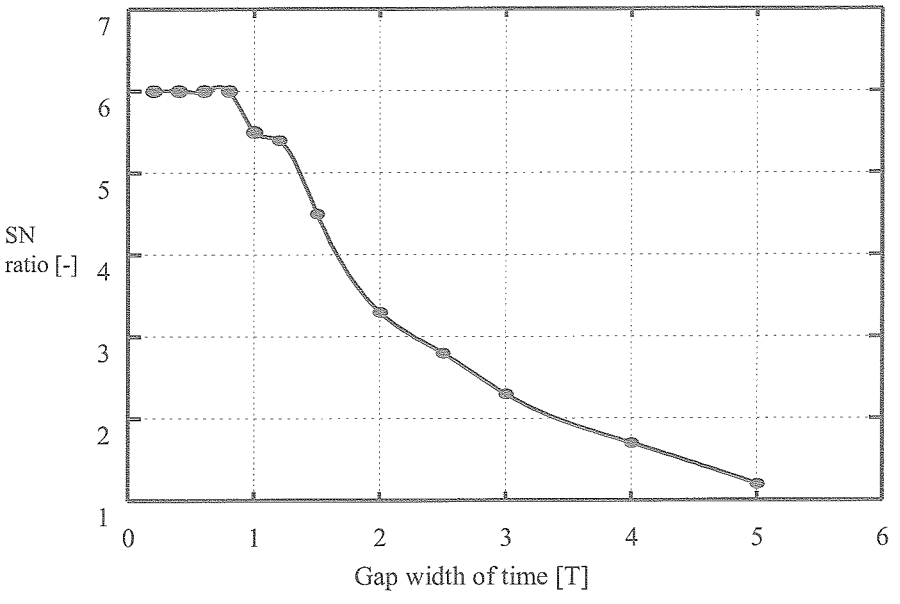

Fig.3-3 Relation between the improvement value in the SN ratio by addition processing, and the time fluctuation value of data

Furthermore, in order to strengthen the ultrasonic echo, the tracer of large size of 300-500 μm was developed. The echo intensity of the large size target that performed signal processing is shown in Fig. 3-4.

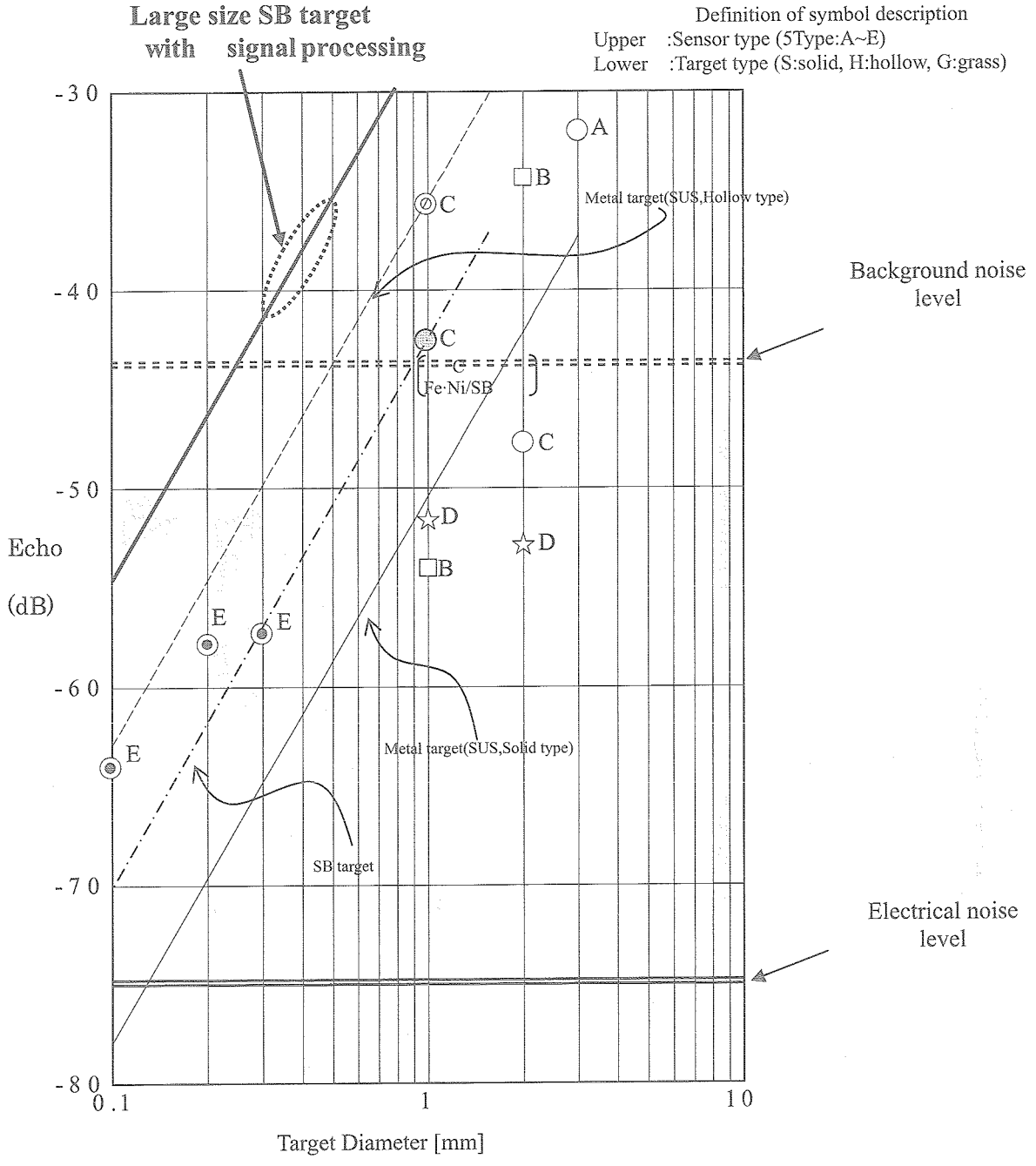

Normalized echo intensity := (echo level)/A/T
A (Sensor sensitivity) :Echo level of sensor head
T :1-R^2 (Transmittance of sound pressure at surface between medium and sensor head)
R(Reflectance of sensor head) :Echo level of surface between medium and sensor head /Echo level of sensor head

Fig.3-4 Prediction of echo intensity of SB

3.1.2 Development for 3D-UV Measuring Unit

Ongoing design of 3D-UV measuring unit is briefly described in this section. The conceptual diagram of a 3D-UV measurement unit is shown in Fig. 3-5. The 3×3 element transducer with a frequency of 10MHz, transmitting and receiving amplifier units are already make ending. This fiscal year made the A/D converter and the system controller.

The signal processing unit made in the Fig. 3-6 is shown. The A/D converter considers as eight channels corresponding to the multi-element transducer, a sampling bit is 12 bits, a sampling frequency is 100MHz, and a loading memory per channel is 64 M bytes. The system controller has the function to perform continuation extraction of measurement data, and transmission to the external personal computer of extraction data, and data transmission speed is 1 Gbit/sec (effective value: about 0.5 Gbit/sec) in a theoretical value. Equalization processing is processed at high speed by FPGA (Field Programmable Gate Array) on A/D converter boards. Data is transmitted and saved at PC. After subtraction processing, the image of the tracer corresponding to the flow pattern is created by synthetic aperture processing.

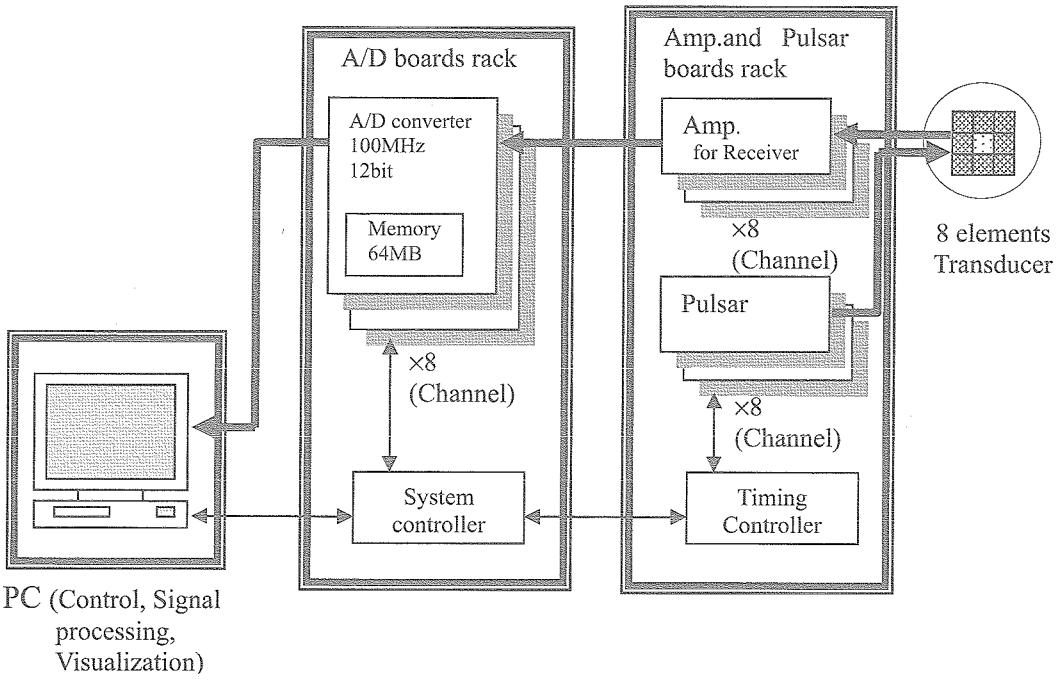

Fig.3-5 Signal processing unit diagram

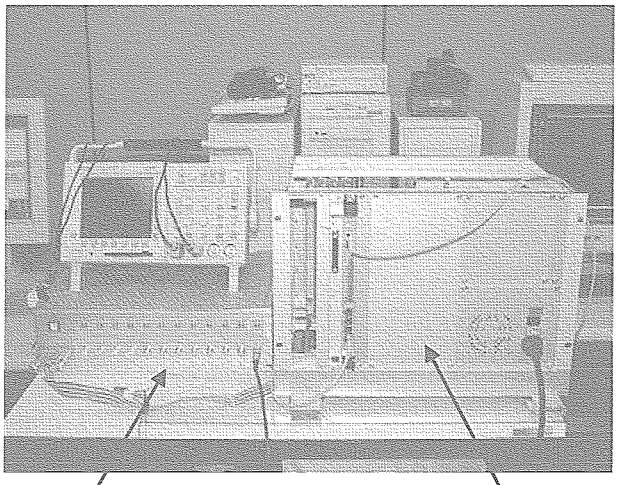

Fig.3-6 Photo. of signal processing unit

4. CONCLUSION

(1) The experimental study on thermocapillary convection of low Prandtl number fluid was carried out to understand transition behavior to oscillatory flow. The half-zone liquid bridge of molten tin was formed between hot and cold disks in high vacuum chamber (10^{-5} Pa). The three radiation thermometers were used to measure the free surface temperature at a different azimuthal location at the same time. In addition, the temperature distribution at interface between liquid bridge and cold disk was measured by using very fine thermocouples. In order to detect the transition point and to make clear the oscillation mode more precisely, the temperature measurement system was developed..

(2) It could be detected that the steady thermocapillary convection changes to oscillatory under certain condition. The observed phenomena of transition processes after the oscillatory onset were revealed by comparing to numerical result done by Imaishi *et al.*. The effect of aspect ratio (L/r) on critical Marangoni number was investigated. The critical Marangoni number decreases with increasing the aspect number. This behavior agrees with numerical simulation done by Imaishi *et al.* qualitatively except for region of smaller aspect ration.

(3) Since the echo signal from the tracer had the very small bad SN ratio, in order to raise the SN ratio, signal processing technique was examined. Consequently, the noise which originates in the shoe by the subtraction processing technique was removable. And the SN ratio could be improved by the addition processing by repetition measurement, and the SN ratio improved about 3 times by calculation supposing actual measurement. The A/D converter and the system controller were manufactured in the 3D-UV measurement unit.

References

[1] H. Kuhlmann, in: Hydrodynamic Instabilities in Thermocapillary Flows, Microgravity Science Technology VII/2 (1994) 75.

[2] N. Imaishi, S. Yasuhiro, T. Sato, and S. Yoda, in: Proc. 44th SPIE Annual Meeting and Exhibition, Materials Research in Low Gravity II, Denver, **3792** (1999) 344.

[3] N. Imaishi, S. Yasuhiro, and S. Yoda, in: Marangoni Convection Modeling Research Annual Report (NASDA-TMR-000006E), National Space Development Agency of Japan (2000) 157.

[4] S. Nakamura, T. Hibiya, K. Kakimoto, N. Imaishi, S. Nishizawa, A. Hirata, K. Mukai, S. Yoda, and T. Morita, J. Crystal Growth, **186** (1998) 85.

[5] T. Hibiya, S. Nakamura, N. Imaishi, K. Mukai, K. Onuma, P. Dold, A. Cröll, K-W. Benz, and S. Yoda, in: Proc. Joint 1st Pan-Pacific Basin Workshop and 4th Japan-China Workshop on Microgravity Sciences, Tokyo (1998) 8.

[6] J. Han, Z. Sun, L. Dai, J. Xie, and W. Hu, J. Crystal Growth, **169** (1996) 129.

[7] Y.K. Yang and S. Kou, J. Crystal Growth, **222** (2001) 135.

[8] R. Imai, K. Takagi, M. Ohtaka, F. Ohtsubo, H. Natsui, and S. Yoda, in: Marangoni Convection Modeling Research Annual Report (NASDA-TMR-990007E), National Space Development Agency of Japan (1999) 71.

[9] K. Takagi, M. Ohtaka, H. Natsui, T. Arai, and S. Yoda, in: Marangoni Convection Modeling Research Annual Report (NASDA-TMR-000006E), National Space Development Agency of Japan (2000) 115.

[10] K. Takagi, M. Otaka, H. Natsui, T. Arai, S. Yoda, Z. Yuan, K. Mukai, S. Yasuhiro, and N. Imaishi, J. Crystal Growth, **233** (2001) 399

[11] M. Ohtaka, K. Takagi, H. Natsui, T. Arai, and S. Yoda, in: Proc. 2nd Pan-Pacific Basin Workshop on Microgravity Sciences, Pasadena (2001) IF-1159.

[12] K. Takagi, M. Otaka, H. Natsui, T. Arai, and S. Yoda, J. Jpn. Soc. Microgravity Appl. (in Japanese), **18** (2001) 11.

[13] N. Imaishi, S. Yasuhiro, Y. Akiyama and S. Yoda, J. Crystal Growth, **230** (2001) 164

[14] Z.Yuan, K.Mukai, K.Takagi and M.Ohtaka, J.Jpn. Inst. Metals (in Japanese), **65** (2001) 21.

[15] A. Passerone, E.Ricci and R.Sangiorgi, J. Material Sci., **25** (1990) 4266

[16] R.Sangiorgi, C.Senillou and J.C.Joud, Surface Sci., **202** (1988) 509

[17] M. Ohtaka, K. Takagi, H. Natsui, T. Arai, and S. Yoda, in: Marangoni Convection Modeling Research Annual Report (NASDA-TMR-010015E), National Space Development Agency of Japan (2001) 145.

[18] M. Matsumoto, M. Ohtaka, H. Natsui, T. Arai, and S. Yoda, in: Marangoni Convection Modeling Research Annual Report (NASDA-TMR-020026E), National Space Development Agency of Japan (2002) 157.

[19] M. Matsumoto, H. Hayashida, A. Komiya, H. Natsui, T. Arai, and S. Yoda, in: Marangoni Convection Modeling Research Annual Report (NASDA-TMR-030004E), National Space Development Agency of Japan (2003) 159.